

SCATTERING BY BEADED HELICES: ANISOTROPY AND CHIRALITY

VIJAY K. VARADAN, AKHLESH LAKHTAKIA and VASUNDARA V. VARADAN
Department of Engineering Science & Mechanics
and
The Center for Engineering of Electronic and Acoustic Materials
The Pennsylvania State University
UNIVERSITY PARK, PA 16802.

ABSTRACT

The field scattered by beaded helices is explored by modeling the individual beads as point dipoles and using multiple scattering theory to account for the interactions between the beads. Whereas the beads are also sufficiently small to be modelled as point dipoles, the overall size of the finite helical arrangement can be large enough to be in the high-frequency regime. The beads have been chosen to be prolate spheroids so that the possible effects of anisotropy on chirality can be studied. From the computed results it is shown

1. INTRODUCTION

In an earlier communication [1], we have described the response of a beaded helix to incident electromagnetic radiation. The helix could be either left-handed or right-handed, and it consisted of spherical beads strung out on an imaginary helical strand. Whereas the beads were sufficiently small to be modelled as point dipoles, the overall size of the finite helical arrangement could be large enough to be even in the high-frequency regime. Furthermore, the beads were chosen to be spherical so that the polarizability tensor of rank one could be used, and the effects of anisotropy thus discarded. From the computed results it can be shown that the dipole-dipole interactions between the beads are the primary contributors to the handedness in the scattered field. A secondary contributor turns out to be the simply the geometry of the helical ensemble of the beads, but which contributes merely to a rotation of the scattering pattern, and that too, not at low frequencies.

Here we are interested in exploring the possible effects of anisotropy on chirality. For this purpose, we have chosen the beads to be prolate spheroids, so that their electric polarizability tensor (of rank 2) gives rise to anisotropic effects. By comparing the responses of spherical and prolate spheroidal beads of identical maximum dimension, the influence of anisotropy is evaluated.

2. FIELD SCATTERED BY A BEADED HELIX

The helix on which the beads are located is given, in a cartesian co-ordinate system, by the radius vector

$$\mathbf{r}(\varphi) = a [\mathbf{i} \cos\varphi + \mathbf{j} h \sin\varphi] + k P (\varphi / 2\pi), \quad \varphi \in \{-\infty, \infty\}, \quad (1)$$

where a is the radius and P is the pitch of the helix; the handedness parameter $h = +1$ if the helix curls up in the $+z$ direction according to the right-handed rule, and $h = -1$, if otherwise. The identical beads are arranged on this helical coil as follows: Let the helix be finite in extent, having $2N+1$ complete rotations so that φ extends over the range $\{-(2N+1)\pi, (2N+1)\pi\}$, N being a positive integer or zero. On each of the $2N+1$ rings of this finite helix, there are $2M+1$ beads arranged over equal $\Delta\varphi$ segments, M being a positive integer greater than zero. Then, the position vector of the m^{th} bead on the helix is given as

$$\mathbf{r}_m = a [\mathbf{i} \cos\varphi_m + \mathbf{j} h \sin\varphi_m] + k P (\varphi_m / 2\pi), \quad m \in \{1, Q\}, \quad (2a)$$

where

$$\phi_m = \pi(2m - Q - 1) / (2M + 1), \quad (2b)$$

$$Q = (2N + 1)(2M + 1). \quad (2c)$$

It is to be noted that the beads in this arrangement are small enough that no two of them ever touch.

Insofar as the electromagnetic properties of the beads are concerned, they possess a dielectric constant ϵ , and if a field \mathbf{E}_m illuminates the m^{th} bead, an electric dipole moment [2]

$$\mathbf{p}_m = \boldsymbol{\alpha}_m \cdot \mathbf{E}_m \quad (3)$$

is induced on it, with $\boldsymbol{\alpha}_m$ being the isotropic electric polarizability tensor [2] of the m^{th} bead in the global cartesian co-ordinate system. This induced dipole moment then re-radiates, the re-radiated field being given as [3]

$$4\pi\epsilon_0 \mathbf{E}_{\text{rad},m}(\mathbf{r}) = \left[k^2 (\mathbf{n}_m \times \mathbf{p}_m) \times \mathbf{n}_m + [3\mathbf{n}_m (\mathbf{n}_m \cdot \mathbf{p}_m) - \mathbf{p}_m] \right. \\ \left. \times (R_m^{-2} - jkR_m^{-1}) \right] \exp(jkR_m) / R_m, \quad (4)$$

where

$$R_m = |\mathbf{r} - \mathbf{r}_m|, \quad (5a)$$

$$\mathbf{n}_m = (\mathbf{r} - \mathbf{r}_m) / R_m. \quad (5b)$$

A magnetic dipole is also induced on each of the Q beads, as also are the higher-order multipoles [3]; however, the maximum bead dimension is sufficiently small that (3) and (4) suffice to describe the scattering response of the m^{th} bead.

The electric polarizability tensor $\boldsymbol{\alpha}_m$ is dependent not only on the location and the properties of the m^{th} bead but on its shape as well. This tensor is well-known for several shapes [2], and in [1] we have already used it for spherical shapes for which bodies it can be thought of simply as a scalar. Since our interest now lies in evaluating the effect of anisotropy in chirality, we have chosen the beads to be prolate spheroidal in shape. The procedure for determining $\boldsymbol{\alpha}_m$ is now described.

Three mutually orthogonal unit vectors \mathbf{u}_1 , \mathbf{u}_2 and \mathbf{u}_3 are prescribed on the helical strand described by Eq. (1). The first of these is tangential to the helix, while \mathbf{u}_2 and \mathbf{u}_3 are normal to it; they are given at \mathbf{r}_m by the transformation

$$\begin{bmatrix} \mathbf{u}_1 \\ \mathbf{u}_2 \\ \mathbf{u}_3 \end{bmatrix} = \begin{bmatrix} (-a/M)\sin\phi_m & (ha/M)\cos\phi_m & P/2\pi M \\ \cos\phi_m & h\sin\phi_m & 0 \\ (hP/2\pi M)\sin\phi_m & (-P/2\pi M)\cos\phi_m & ha/M \end{bmatrix} \begin{bmatrix} \mathbf{i} \\ \mathbf{j} \\ \mathbf{k} \end{bmatrix} = [\mathbf{C}_m] \begin{bmatrix} \mathbf{i} \\ \mathbf{j} \\ \mathbf{k} \end{bmatrix} \quad (7)$$

The m^{th} bead is so placed that its major axis is aligned on the tangential vector \mathbf{u}_1 at \mathbf{r}_m , as shown in Fig. 1. Working with these three unit vectors, (3) turns out to be [2]

$$\mathbf{p}_m \cdot \mathbf{u}_i = g_i \mathbf{E}_m \cdot \mathbf{u}_i, \quad i = 1, 2, 3 \quad (8a)$$

with

$$g_1 = (4/3)[\pi\epsilon_0 b d^2] (\epsilon/\epsilon_0 - 1) \left(L(\epsilon/\epsilon_0 - 1) + 1 \right)^{-1}, \quad (8b)$$

$$g_2 = g_3 = (4/3)[\pi\epsilon_0 b d^2] (\epsilon/\epsilon_0 - 1) \left((1/2)(1-L)(\epsilon/\epsilon_0 - 1) + 1 \right)^{-1}, \quad (8c)$$

$$L = 1 + 2f^{-2}(1-f^2) \left\{ 1 - (2f)^{-1} \log_e[(1+f)(1-f)^{-1}] \right\}, \quad (8d)$$

$$f^2 = 1 - (d/b)^2, \quad (8e)$$

where b is the semi-major dimension of the prolate spheroidal beads, and d their equatorial radius. On substituting (7) into (8a) in order to get a polarizability tensor for the m^{th} bead in the cartesian co-ordinate system, we get

$$\underline{\alpha}_m = [C_m]^{\text{tr}} \begin{bmatrix} g_1 & 0 & 0 \\ 0 & g_2 & 0 \\ 0 & 0 & g_3 \end{bmatrix} [C_m], \quad (9)$$

the superscript 'tr' denoting the transpose. It should be noted that were $b = d$, i.e., if the beads were to be spherical, then $L = 1/3$ and $g_1 = g_2 = g_3$. Also, despite the fact that all of the spheroidal beads are identical, the various $\underline{\alpha}_m$ are not because the three unit vectors u_1 , etc. differ for differing r_m .

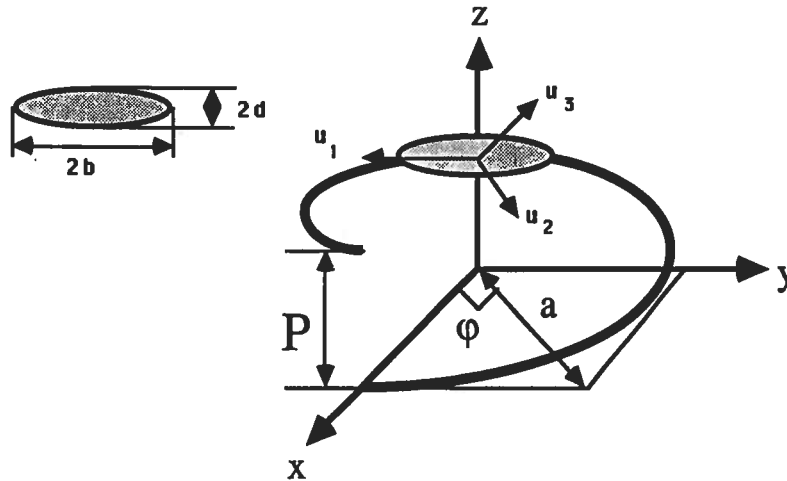


Figure 1 Schematic of the helical strand on which the prolate spheroidal beads are strung.

The electromagnetic field incident on the helix is taken here to be the circularly polarized planewave,

$$E_{\text{inc}}(\mathbf{r}) = (\mathbf{i} \pm j \mathbf{j}) \exp[j \mathbf{k} \cdot \mathbf{r}], \quad (10)$$

where the '+' (resp. '-') in the polarization of E_{inc} indicates that it is right- circularly (resp. left-circularly) polarized as it propagates in the $+z$ direction. But the field E_m actually incident on the m^{th} bead is not

$E_{\text{inc}}(\mathbf{r}_m)$ alone; it also consists of the fields $E_{\text{rad},n}(\mathbf{r}_m)$, $\forall n \neq m$, re-radiated by all of the other beads as well [4], [5]. It is then easy to see that the field exciting the m^{th} bead can be self-consistently written as

$$\mathbf{E}_m = \mathbf{E}_{\text{inc}}(\mathbf{r}_m) + \sum_{n, n \neq m} \mathbf{E}_{\text{rad},n}(\mathbf{r}_m). \quad (11)$$

Using now (3), (4) and (9) in (11), the system of $3Q$ simultaneous equations,

$$\mathbf{E}_m = \mathbf{E}_{\text{inc}}(\mathbf{r}_m) + k^2(4\pi\epsilon_0)^{-1} \sum_{n, n \neq m} \left\{ \mathbf{R}_{mn}^{-1} \exp(jkR_{mn}) [g_{mn} \mathbf{n}_{mn} (\mathbf{n}_{mn} \cdot \mathbf{p}_n) - h_{mn} \mathbf{p}_n] \right\}, \quad (12)$$

must be solved, in order to obtain the various exciting fields \mathbf{E}_m . In (12),

$$R_{mn} = |\mathbf{r}_m - \mathbf{r}_n|, \quad (13a)$$

$$\mathbf{n}_{mn} = (\mathbf{r}_m - \mathbf{r}_n) / R_{mn}, \quad (13b)$$

$$g_{mn} = 3(kR_{mn})^{-2} - 3j(kR_{mn})^{-1} - 1, \quad (13c)$$

$$h_{mn} = (1/3) [g_{mn} - 2]. \quad (13d)$$

Once the solution of (12) has been obtained, the total scattered field outside the circumscribing sphere can be computed simply as [3 - 5]

$$4\pi\epsilon_0 \mathbf{E}_{\text{sc}}(\mathbf{r}) = \sum_m \left[\{k^2(\mathbf{n}_m \times \mathbf{p}_m) \times \mathbf{n}_m + [3\mathbf{n}_m(\mathbf{n}_m \cdot \mathbf{p}_m) - \mathbf{p}_m] (R_m^{-2} - jkR_m^{-1})\} \exp(jkR_m) / R_m \right], \quad (14)$$

which, for $kr \rightarrow \infty$, can be simplified to [3]

$$4\pi\epsilon_0 \mathbf{E}_{\text{sc}}(\mathbf{r}) = k^2 r^{-1} \exp(jkr) \sum_m \left\{ \exp(-jkr_m \cdot \mathbf{r} / r) (\mathbf{p}_m - \mathbf{r} (\mathbf{r} \cdot \mathbf{p}_m) / r^2) \right\}. \quad (15)$$

It is again emphasized here that, in deriving (14), there are no restrictions placed either on the radius a or on the pitch P of the helix; the only limitation here is that the beads be sufficiently small so that their scattering response can be adequately described via (3) and (4).

3. NUMERICAL RESULTS AND DISCUSSION

Equations (12) and (15) were programmed on a DEC VAX 11/730 minicomputer and the exciting fields \mathbf{E}_m as well as the scattering pattern $\mathbf{F}_{\text{sc}}(\theta, \phi) = (r \exp[-jkr]) \mathbf{E}_{\text{sc}}(r, \theta, \phi)$ as $kr \rightarrow \infty$ were computed for the right- and the left-circularly polarized planewaves incident in a direction parallel to the $+z$ axis. The angles θ and ϕ , respectively are the inclinations of the vector \mathbf{r} from the $+z$ axis in any longitudinal plane, and from the $+x$ axis in the xy plane.

It was mentioned earlier that the dipole-dipole interactions appear to be the primary contributors to the handedness of the response of the beaded helices. From our computations made with the prolate spheroidal beads, it turns out that there are several intertwining factors that affect the dipole-dipole interactions, and, thus, the ability of a given helix to discriminate between the right-circularly polarized (RCP) and the left-circularly polarized (LCP) planewaves. First of all, if the relative dielectric constant ϵ/ϵ_0 of the beads increases, they become more efficient scatterers since $|\mathbf{p}_m|$ increases; there is, no doubt, a maximum limit on ϵ/ϵ_0 for the available materials. Secondly, if the beads are larger in size, then too the scattering efficiency increases, and for the same reason. But the maximum permissible bead size is regulated by both the radius a and the pitch P of the helix. It is clear that larger helical radii will permit larger beads, or alternatively,

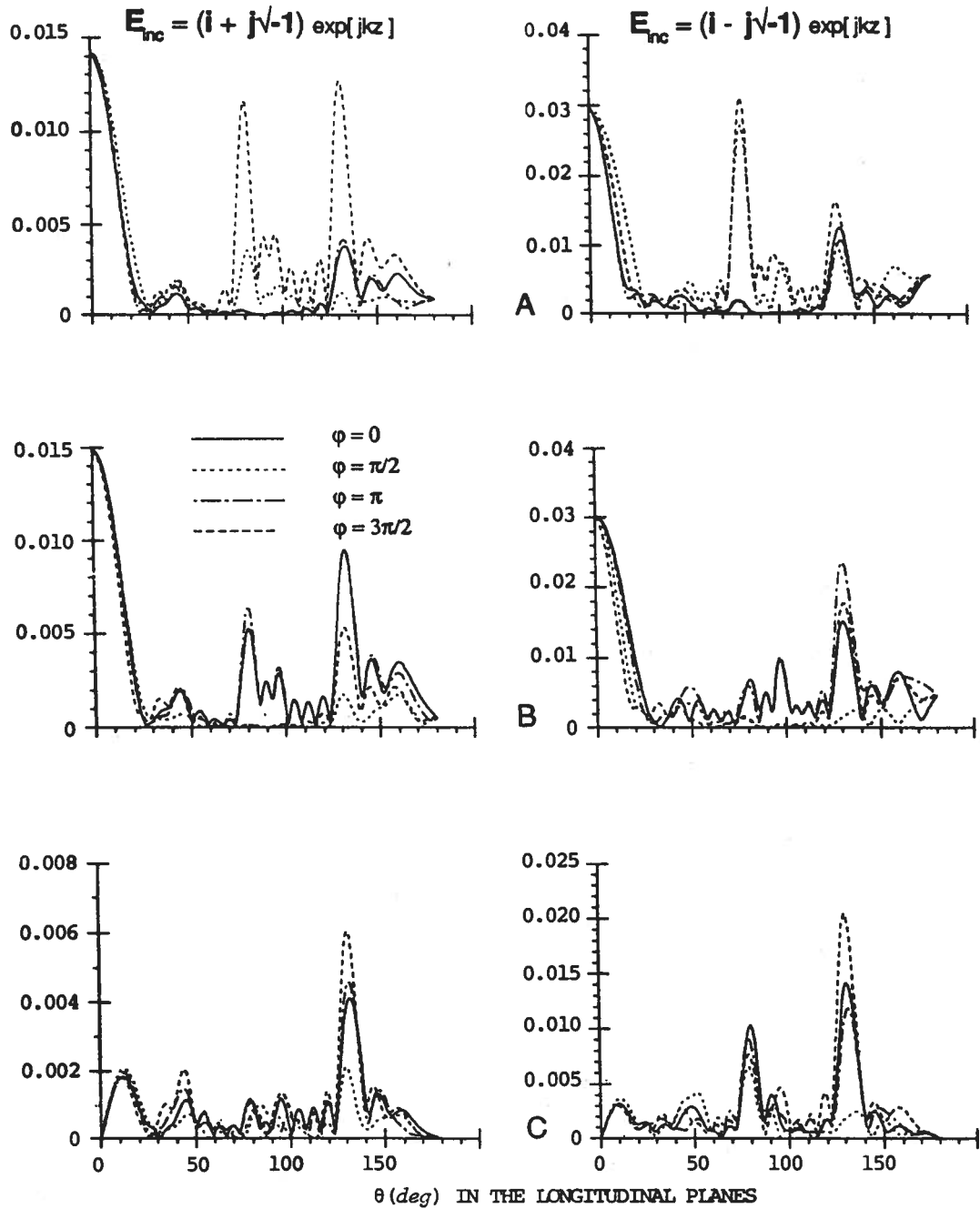


Figure 2 Magnitudes of the components of the scattering pattern $F_{sc}(\theta, \varphi)$ are plotted in several longitudinal planes for a right-handed helix ($h = +1$) on which 35 prolate spheroidal beads have been strung. The parameters $N = 2$, $M = 3$; $a = 0.002$ m, $P/a = 0.003$ m, $b = 1.25664 \times 10^{-3}$ m, $d = b/3$, $\epsilon/\epsilon_0 = 4.0$; and $ka = 5.0$. (a) The x-directed component, (b) the y-directed component, and (c) the z-directed component. The incident plane wave is given by (10).

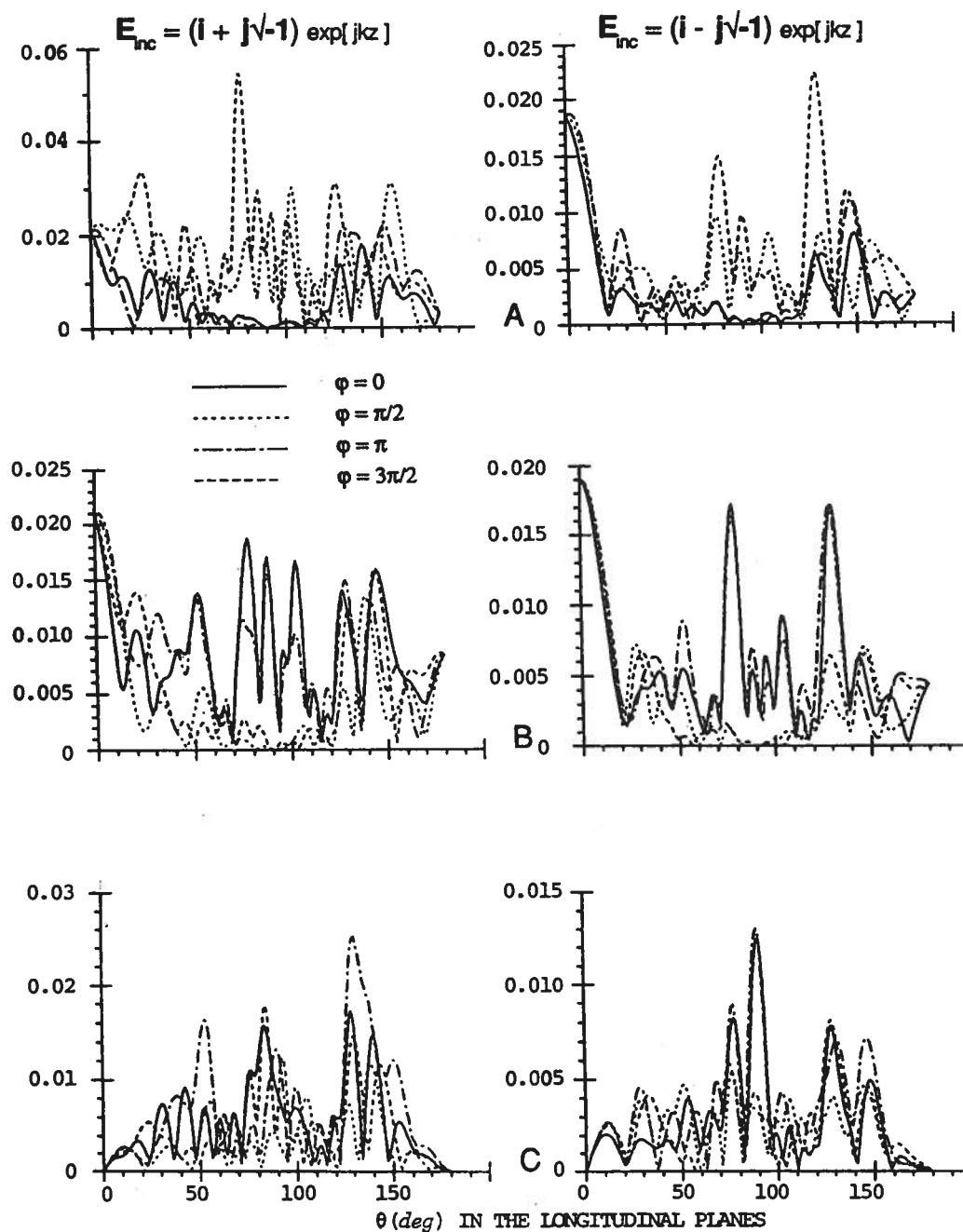


Figure 3 Same as Fig. 2, except $d = b$ so that the beads are spherical and α_m can be represented by a scalar $\alpha = (4\pi\epsilon_0 b^3) (\epsilon/\epsilon_0 - 1)(\epsilon/\epsilon_0 + 2)^{-1}$ for all the beads.

simply more beads, either of which eventuality will accentuate the dipole-dipole interaction. On the other hand, the maximum permissible bead size certainly decreases if the helix is more tightly wound, i.e., P increases; but the consequent decrease in the scattering efficiency of the individual bead may be offset by the proximity to each other of the beads in the consecutive rings, which will strengthen the dipole-dipole interactions.

Frequency also plays a major role in influencing the discriminatory ability of the helices. It is well-known [6] that the scattered field in the near zone of a scatterer is considerably more chaotic than in the far zone, this being due to the fact that the near zone field contains large, reactive components. In the far zone, the field decays inversely with distance from the scatterer and does not contain any significant amount of reactive components. Higher, however, the frequency, smaller is the near zone expanse in meters. Therefore, if the beads are strung too far apart from each other, because either the helix radius or the pitch is large in relation to the ambient wavelength, the dipole-dipole interaction is less effective. For a specified helix, then, the interactions should be more pronounced: at the lower frequencies, however, the beads re-radiate less efficiently.

From these considerations it appears that if the number $(2M+1)$ of the beads per ring is small, the bead size parameter kb is large, and both a and P are of the order of the ambient wavelength, one can expect the circular polarization-discriminatory ability of the helix to be the most pronounced. This indeed turns out to be the case, both from our calculations as well as of others [e.g. 7].

Shown in Fig. 2 are the magnitudes of the cartesian components of scattering pattern $F_{sc}(\theta, \varphi)$ in several longitudinal planes for a right-handed helix ($h = +1$) on which 35 prolate spheroidal beads have been strung; the parameters $N = 2$, $M = 3$; $a = 0.002$ m, $P/a = 0.003$ m, $b = 1.25664 \times 10^{-3}$ m, $d = b/3$, $\epsilon/\epsilon_0 = 4.0$; and $ka = 5.0$. A cursory glance at this figure tells us that the helix has been able to discriminate quite effectively between the incident RCP and LCP planewaves. Precisely the same conclusion can be drawn from Fig. 3 where the beads are spherical so that $b = d = 1.25664 \times 10^{-3}$ m and the electric polarizability tensor is isotropic; the calculations were performed using the procedure outlined in [1]. In general, however, the scattering efficiency of the helix is more when the beads are spherical, this being due to the fact that the bead volume then is greater and for particles (i.e., beads) much smaller than the ambient wavelength, scattering efficiency varies with the particle volume.

A more interesting comparison, however, is that of the value of $F_{sc}(0, \varphi)$. In Fig. 2, when the beads are prolate spheroids of aspect ratio 3:1, then $|F_{sc}(0, \varphi)| \approx 0.0205$ for the incident RCP planewaves, and $|F_{sc}(0, \varphi)| \approx 0.0425$ for the incident LCP planewave. This certainly means that the right-handed helix made up of prolate spheroidal beads, aligned as in Fig. 1, guides the RCP planewave about itself and does not remove as much energy from it as it does from the LCP planewave, which it scatters more. Thus, the right-handed helix acts as a guiding structure for the incident RCP excitation; the elongated beads arranged tangentially to the helix serving as conduits. In Fig. 3, however, the beads are spherical and anisotropy in the electric polarizability is absent; thus the magnitudes of the cartesian components of $F_{sc}(0, \varphi)$ are about the same for the specified planewave incidence of either polarization. Actually, $|F_{sc}(0, \varphi)| \approx 0.0283$ for RCP incidence, and $|F_{sc}(0, \varphi)| \approx 0.0275$ for LCP incidence. This difference is small, but it means that the guiding structure present in the helix of Fig. 3 is absent here because of the fact that scattering is due to isotropic, point-polarizable scatterers.

REFERENCES

1. V.V. Varadan, A. Lakhtakia and V.K. Varadan, "Equivalent dipole moments of helical arrangements of small, isotropic, point-polarizable scatterers: Application to chiral polymer design," *J. Appl. Phys.* (accepted for publication).
2. H.C. van de Hulst, *Light Scattering by Small Particles*, New York: Wiley (1957).
3. J.D. Jackson, *Classical Electrodynamics*, New York: McGraw-Hill (1975).
4. E.M. Purcell and C.R. Pennypacker, "Scattering and absorption of light by nonspherical dielectric grains," *Astrophys. J.* **186**, 705-714 (1973).

5. V.K. Varadan, "Multiple scattering of acoustic, electromagnetic and elastic waves," in *Acoustic, Electromagnetic and Elastic Wave Scattering* (V.K. and V.V. Varadan, Eds.), New York: Pergamon, (1980).
6. A. Lakhtakia, M.F. Iskander, C.H. Durney and H. Massoudi, "Near-field absorption in prolate spheroidal models of humans exposed to a small loop antenna of arbitrary orientation," *IEEE Trans. Microwave Theory Tech.* **29**, 588-593 (1981).
7. S.B. Singham and G.C. Salzman, "Evaluation of the scattering matrix of an arbitrary particle using the coupled dipole approximation," *J. Chem. Phys.* **84**, 2658-2667 (1986).